

An excursion set model for the distribution of dark matter and dark matter haloes

Ravi K. Sheth^{*}

Max-Planck Institut für Astrophysik, Karl-Schwarzschild-Strasse 1, 85740 Garching, Germany

Accepted 1998 July 9. Received 1998 June 23; in original form 1997 September 26

ABSTRACT

A model of the gravitationally evolved dark matter distribution, in the Eulerian space, is developed. It is a simple extension of the excursion set model that is commonly used to estimate the mass function of collapsed dark matter haloes. In addition to describing the evolution of the Eulerian space distribution of the haloes, the model allows one to describe the evolution of the dark matter itself. It can also be used to describe density profiles, on scales larger than the virial radius of these haloes, and to quantify the way in which matter flows in and out of Eulerian cells. When the initial Lagrangian space distribution is white noise Gaussian, the model suggests that the Inverse Gaussian distribution should provide a reasonably good approximation to the evolved Eulerian density field, in agreement with numerical simulations. Application of this model to clustering from more general Gaussian initial conditions is discussed at the end.

Key words: methods: analytical – galaxies: clusters: general – galaxies: formation – cosmology: theory – dark matter.

1 INTRODUCTION

The hypothesis that, in comoving coordinates, initially denser regions contract more rapidly than less dense regions, and that sufficiently underdense regions expand, is simple, reasonable, and powerful. As a consequence of this expansion and contraction, the density distribution in the initial Lagrangian space will be different from that in the evolved, Eulerian space. Suppose that, as the Universe evolves, the number of expanding and contracting regions is conserved – only their comoving size changes – and the mass within each such region is also conserved. If we have a model for the way in which the evolution of the size of a region depends on its initial size and density, and we also have a model for the initial number of regions as a function of initial size and density, then we can compute the distribution of sizes and densities at some later time. For example, suppose that the initial Lagrangian density distribution is a Gaussian random field, and that the evolution of regions is given by the spherical collapse model. Then it should be possible to construct a model for $p(M_0|R, z)$, where $p(M_0|R, z)$ is the fraction of regions of size R that, at z , contain mass M_0 . The quantity $p(M_0|R, z)$ is often called the Eulerian probability distribution function.

In the Press–Schechter (1974) approach, at any given time, all matter is in the form of collapsed objects, usually called haloes, and the distribution of halo masses evolves with time. At any time, the matter within a randomly placed cell R is divided among many

collapsed haloes. Thus, $p(M_0|R, z)$ depends both on the halo mass function, and on the spatial distribution of the haloes. Bond et al. (1991) showed how to estimate the evolution of the halo mass function if the initial Lagrangian distribution is Gaussian (also see Lacey & Cole 1993). They did not show how to estimate the spatial distribution of these haloes, but Mo & White (1996) showed how this might be accomplished. This paper develops a model that combines, self-consistently, the Bond et al. excursion set approach with the Mo & White model for the Eulerian space halo distribution. The model developed here allows one to simultaneously describe both the distribution of the dark matter, i.e., $p(M_0|R, z)$, and that of the haloes. See, e.g., Mo & White (1996) for why such a model is useful.

Section 2 describes the model. It shows why the distribution of first crossings of a barrier whose height is not constant, by Brownian motion random walks, is useful. The shape of the barrier associated with the spherical collapse model is given in Section 2.2. The relation between the first-crossing distribution and the Eulerian distribution $p(M_0|R, z)$ is discussed in Section 2.3. Section 2.4 shows that, in the context of the model developed here, the halo mass function is related to the small cell size limit (i.e., $R \rightarrow 0$) of $p(M_0|R, z)$. It discusses the Bond et al. (1991) excursion set results in this context, and then shows how the model can be used to describe the spatial distribution of the haloes as well. The results of Mo & White (1996) are discussed in Section 2.5. Section 2.6 shows that the associated two-barrier problem can be used to provide information about the evolved density profile, and also about the way in which matter flows in and out of Eulerian cells.

^{*}E-mail: sheth@mpa-garching.mpg.de

The first-crossing distribution associated with the spherical collapse barrier must be obtained numerically. Therefore, to illustrate the usefulness of our approach, Section 3 shows the results of assuming that the initial distribution is white-noise Gaussian, and that the barrier shape is simpler than that associated with the spherical collapse model. In Section 3, the barrier is assumed to be linear for a number of reasons. First, this linear barrier can be understood as arising from a simple variant of the spherical collapse model (Section 3.1). Secondly, the barrier-crossing distribution can be computed analytically (e.g. Schrödinger 1915). The details of the derivation are presented in Appendix A. Thirdly, the Eulerian probability distribution associated with the first crossings of this linear barrier is Inverse Gaussian (Section 3.3), and the Inverse Gaussian provides a good fit to the Eulerian distribution measured in numerical simulations of clustering from white-noise initial conditions (Section 3.6). Finally, studies of clustering from Poisson initial conditions also suggest that this barrier shape is a useful approximation (Sheth 1998).

The Bond et al. (1991) results are derived, within the context of this linear barrier model, in Section 3.2. Analytic expressions for the Eulerian distribution function as well as the halo–mass and halo–halo correlations are derived for all scales, and for all times, in Sections 3.3 and 3.4. Section 3.5 provides various formulae associated with the two-linear-barrier problem. Section 4 discusses some scaling properties of the model, and also how the model can be extended to describe clustering from more general initial conditions. Section 5 summarizes the results.

2 THE EXCURSION SET MODEL

The first subsection defines various Eulerian space quantities of interest in this paper. Since these definitions are standard (e.g. Peebles 1980), no further references are given. Subsequent subsections develop a model which allows one to estimate the evolution of these quantities.

2.1 The matter and halo distribution in Eulerian space

Imagine partitioning the Eulerian space V_{tot} into a large number of cells, each of size $V \equiv (4\pi/3)R^3$, at time z . Since the volume of each cell is V , the total number of such cells is $N_{\text{tot}} = V_{\text{tot}}/V$. Let $p(M_0|R, z) dM_0$ denote the fraction of these cells that contain mass between M_0 and $M_0 + dM_0$. Then, at a given z ,

$$p(M_0|R, z) dM_0 = \frac{N(M_0|R) dM_0}{N_{\text{tot}}} = \frac{V N(M_0|R) dM_0}{V_{\text{tot}}}, \quad (1)$$

where we have not bothered to write z explicitly on the right-hand side. Define $\Delta \equiv (1 + \delta) \equiv M_0/\bar{\rho}V$, where $\bar{\rho}$ is the average comoving density in the Eulerian space. That is,

$$\bar{\rho} = \frac{M_{\text{tot}}}{V_{\text{tot}}} = \frac{1}{V_{\text{tot}}} \int_0^\infty M_0 N(M_0|R, z) dM_0. \quad (2)$$

Then

$$p(\Delta|R, z) d\Delta = p(M_0|R, z) dM_0, \quad (3)$$

and $p(\Delta|R, z)$ is the probability distribution function of the density in Eulerian space at z . Since $d\Delta = dM_0/(\bar{\rho}V)$,

$$\int_0^\infty p(\Delta|R, z) d\Delta = \int_0^\infty \Delta p(\Delta|R, z) d\Delta = 1 \quad (4)$$

for all z .

Let $\bar{n}(M_1, \delta_{c1})$, where $\delta_{c1} = \delta_{c0}(1 + z_1)$ and δ_{c0} is some constant that will be determined later, denote the average number density of

M_1 haloes identified at z_1 . On average, the number of such haloes within an Eulerian cell V is $\bar{n}(M_1, \delta_{c1})V$. Let N_1 denote the number of such M_1 haloes within the i th Eulerian cell. Suppose we classify all Eulerian cells by the mass M_0 within them at some $z < z_1$. Let $N(1|0)$ denote $\langle N_1 \rangle_0$, where the average is over only those Eulerian cells that contain mass M_0 at z . Clearly,

$$\bar{n}(M_1, \delta_{c1})V = \int_0^\infty N(1|0) p(\Delta|R, z) d\Delta, \quad (5)$$

since equation (3) shows that $p(M_0) dM_0 = p(\Delta) d\Delta$.

Define

$$\delta_h(1|0) = \frac{N(1|0)}{\bar{n}(M_1, \delta_{c1})V} - 1. \quad (6)$$

This is the number, relative to the average number of (M_1, δ_{c1}) haloes in Eulerian cells V , of such haloes that are within Eulerian cells which contain mass M_0 at z , minus one. The cross-correlation $\bar{\xi}_{\text{hh}}(M_1, \delta_{c1}|R, z)$ between haloes and mass in Eulerian space, averaged over Eulerian cells of comoving size V , at the epoch z , is

$$\begin{aligned} \bar{\xi}_{\text{hh}}(1|R, z) &= \langle \delta_h(1|0) \delta \rangle_R \\ &= \int_0^\infty (\Delta - 1) \frac{N(1|0) p(\Delta|R, z)}{\bar{n}(M_1, \delta_{c1})V} d\Delta, \end{aligned} \quad (7)$$

where we have used equation (4) to set $\langle \Delta \rangle = \langle 1 + \delta \rangle = 1$, and so $\langle \delta \rangle = 0$.

Let $\bar{\xi}_{\text{hh}}(M_1, M_2, \delta_{c1}|R, z)$ denote the (volume average of the) correlation function of M_1 and M_2 haloes identified at the epoch z_1 , averaged over all comoving Eulerian cells V , at the epoch $z \leq z_1$. This average can be computed in two steps. Let N_1 and N_2 denote the number of M_1 and M_2 haloes within an Eulerian cell V . Classify all Eulerian cells by the mass M_0 within them at z . Let $C(12|0)$ denote the average over all M_0 cells of $\langle N_1 N_2 \rangle$: $C(12|0) \equiv \langle N_1 N_2 \rangle_0$. Then

$$1 + \bar{\xi}_{\text{hh}}(12|R, z) = \int_0^\infty \frac{C(12|0) p(\Delta|R, z)}{\bar{n}(M_1, \delta_{c1})V \bar{n}(M_2, \delta_{c1})V} d\Delta. \quad (8)$$

Higher order moments of the halo distribution can be defined similarly. The remainder of this section develops a barrier-crossing, excursion set model which allows one to estimate all these Eulerian quantities.

2.2 The spherical collapse model

We will assume that the total mass and comoving volume of the evolved Eulerian space are the same as those initially (i.e., in the Lagrangian space). Then the average density in the two spaces is the same: $\bar{\rho}_0 = \bar{\rho}$, where here, and below, quantities with subscript zero are in the Lagrangian space.

We will also assume that the initial over-density fluctuations in the Lagrangian space are small: $\delta_0 \ll 1$ initially. If $\bar{\rho}$ is the average background density, then $M_0 = \bar{\rho}_0 V_0 (1 + \delta_0) \approx \bar{\rho} V_0$, where $V_0 = (4\pi/3)R_0^3$. That is, the initial mass M_0 , volume V_0 and size R_0 are all equivalent variables. Consider a region that initially contains mass M_0 and has initial over-density δ_0 . At some later time, it has size $R(z)$, so that the over-density within it is δ , where

$$1 + \delta \equiv \Delta = M_0/\bar{\rho}V = (R_0/R)^3. \quad (9)$$

Notice that Δ is the same Eulerian quantity of the previous subsection, and that it is simply the ratio of the Lagrangian volume to the Eulerian volume of the region.

The spherical collapse model (e.g. Peebles 1980) allows one to describe the evolution of such a region. In particular, it provides

relations between the initial size R_0 , the initial over-density δ_0 , the time z , and the evolved Eulerian size at that time $R(z)$. If R_0 , δ_0 and z are given, then $R(R_0, \delta_0, z)$ is determined by the model. On the other hand, if only R and z are given, then the model describes a curve in the (R_0, δ_0) plane: $\delta_0(R_0|R, z)$. To a good approximation, this relation is

$$\frac{\delta_0(R_0|R, z)}{1+z} = 1.68647 - \frac{1.35}{\Delta^{2/3}} - \frac{1.12431}{\Delta^{1/2}} + \frac{0.78785}{\Delta^{0.58661}} \quad (10)$$

(Mo & White 1996). A simpler approximation to this relation is

$$\frac{\delta_0(R_0|R, z)}{1+z} = \delta_{c0} - \delta_{c0} \Delta^{-1/\delta_{c0}} \quad (11)$$

(Bernardeau 1994). Whereas Bernardeau used $\delta_{c0} = 1.5$, the value 1.68647 is also acceptable. Since δ_0 is the linear theory density fluctuation, it can be less than -1 . In both these relations, this happens as $\Delta \rightarrow 0$.

Notice that when $R \rightarrow 0$, then $\Delta \rightarrow \infty$, so formulae (10) and (11) both become $\delta_0 \rightarrow \delta_{c0}(1+z)$ with $\delta_{c0} = 1.686$. In this limit $\delta_0(R_0|R=0, z)$ is independent of R_0 . When $R > 0$, then $\delta_0(R_0|R, z)$ decreases monotonically as R_0 decreases. Essentially, equation (10) shows that a given pair R and z could initially have come from a range of R_0 and δ_0 . This is sensible; in the spherical model, initially denser regions collapse more rapidly than less dense regions. Therefore a region of size R at z may initially have been a small region containing a small over-density, or it may have been larger initially, but with a correspondingly larger over-density.

Our model for estimating the Eulerian probability distribution function $p(M_0|R, z)$ works as follows. At any given z , imagine partitioning space into a large number of cells each of size V . Assume that each cell evolved according to the spherical model independently of the others. This means that the mass within each cell remains the same – only its comoving size changes – and the total number of cells is conserved. These are strong simplifying assumptions that, on (larger) scales where shell crossing has yet to occur, are certainly reasonable. In general, however, they do not have a rigorous physical justification. So, as with the Bond et al. (1991) excursion set approach, the extent to which the model here is able to reproduce the results of numerical simulations is, at present, the only real justification for these assumptions. As we show below, these assumptions allow one to estimate a number of useful quantities.

Since each cell evolved according to the spherical model, and the number of such cells is conserved, to compute $p(M_0|R, z)$ we simply need to specify the relative numbers of regions initially with (R_0, δ_0) that have now evolved into regions (R, z) . Clearly, this distribution depends on the initial distribution of fluctuations and on the evolution described by the spherical model. The next subsection shows how to do this.

2.3 The first-crossing distribution

Consider a density field $\delta_0(\mathbf{r}; 0)$. Recall that the subscript zero denotes the fact that δ_0 is a quantity measured in the Lagrangian space. Smoothing this field with a window W of scale R_0 produces a smoothed field $\delta_0(\mathbf{r}; R_0)$:

$$\begin{aligned} \delta_0(\mathbf{r}; R_0) &= \int W(|\mathbf{r} - \mathbf{r}'|, R_0) \delta_0(\mathbf{r}'; 0) d\mathbf{r}' \\ &= \int \bar{W}(k, R_0) \delta_0(k) \exp(i\mathbf{k} \cdot \mathbf{r}) d\mathbf{k}, \end{aligned} \quad (12)$$

where \bar{W} is the Fourier transform of the window W . By definition of the average density, $\delta_0 \rightarrow 0$ as $R_0 \rightarrow \infty$, for all positions \mathbf{r} . Thus, for

each position in the Lagrangian space there is a curve, $\delta_0(R_0)$, which describes the over-density δ_0 in a window of Lagrangian size R_0 centred on that position. Call such a curve a trajectory. The volume associated with a window of size R_0 is $V_0 \equiv V_W R_0^3$, where V_W is some constant that may depend on the shape of the window, but does not depend on R_0 . For example, $V_W = 4\pi/3$ for a top-hat window. The mass within this volume is $M_0 = \bar{\rho}_0 V_0 (1 + \delta_0)$, where $\bar{\rho}_0$ is a constant that denotes the average mass density in the Lagrangian space. Provided the initial δ_0 is small, $M_0 \approx \bar{\rho}_0 V_0$ to lowest order. In this approximation, there is a deterministic relation between the volume V_0 and the mass within it: $M_0 \equiv \bar{\rho}_0 V_0$ in the Lagrangian space.

There is also a deterministic relation between the scale R_0 , and the variance S_0 associated with that scale:

$$S_0 = \langle \delta_0^2(\mathbf{r}; R_0) \rangle = \int P(k) \bar{W}^2(k; R_0) d^3k, \quad (13)$$

where $P(k)$ is the power spectrum of the unsmoothed Lagrangian field. Thus, for a given $P(k)$, the quantities S_0 , R_0 , V_0 and M_0 are equivalent. For most power spectra of interest, S_0 increases as R_0 decreases. For what follows, assume that $S_0 \rightarrow \infty$ as $R_0 \rightarrow 0$.

The deterministic relation between R_0 and S_0 means that to each trajectory $\delta_0(R_0)$ associated with a position in the Lagrangian space, there is a corresponding trajectory $\delta_0(S_0)$. Since $\delta_0(R_0) \rightarrow 0$ as $R_0 \rightarrow \infty$, all these trajectories start from the origin $(S_0, \delta_0) = (0, 0)$. Since $S_0 \rightarrow \infty$ as $R_0 \rightarrow 0$, and since S_0 is a measure of the mean square distance of a trajectory at S_0 from the S_0 axis, any trajectory may be an arbitrary distance above or below the S_0 axis as $R_0 \rightarrow 0$.

The deterministic relation between R_0 and S_0 also means that equation (10) represents a curve in the (S_0, δ_0) space. Given R and z , draw this curve, and call it the barrier $B(S_0|R, z)$. The thick solid curve in Fig. 1 shows this barrier for a representative value of R and z . It decreases monotonically as S_0 increases. For a given z , equation (10) shows that curves for different R all have the same value $B = \delta_{c0}(1+z)$ at $S_0 = 0$. Equation (10) also shows that $B = 0$ when $R = R_0$, so curves for larger values of R cross the S_0 axis at smaller values of S_0 . In fact, for a given z , the curves for different R form a nested family (see Fig. 2). This will be important below.

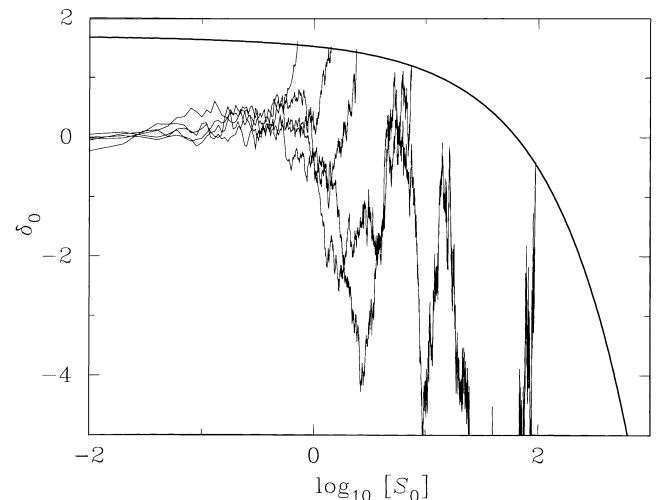


Figure 1. Examples of trajectories (thin jagged curves) traced out by the Lagrangian over-density, δ_0 , as a function of linear variance, S_0 . The trajectories are absorbed at the barrier (thick solid line). Here, the barrier shape is given by the spherical collapse model (equation 10), and $S_0 \propto 1/V_0$ as it is for white noise.

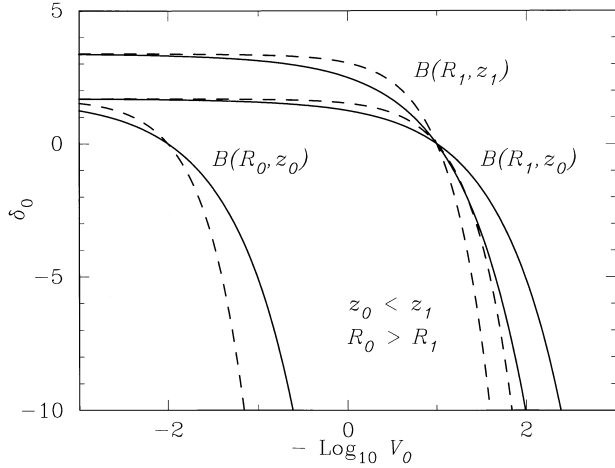


Figure 2. Dependence of the barrier shape on comoving Eulerian size R and redshift z . Solid curves show $B = \delta_0(R_0|R, z)$ of equation (10), and dashed curves show equation (20). For white noise, $S_0 \propto 1/V_0 \propto 1/R_0^3$.

Since $B(S_0|R, z)$ decreases monotonically with increasing S_0 , each Lagrangian trajectory will intersect the barrier at least once (see Fig. 1). Define the first crossing as the smallest value of S_0 at which the Lagrangian trajectory $\delta_0(S_0)$ intersects $B(S_0|R, z)$. That is, it is the smallest S_0 at which $\delta_0 = B$. Bond et al. (1991) discuss why the first-crossing distribution is so important (it solves the so-called cloud-in-cloud problem). Although they only considered the special case in which $B(S_0|R, z)$ was independent of S_0 , their argument holds for the more general barrier considered here also. The argument is as follows.

Consider a trajectory $\delta_0(S_0)$. It may cross the barrier $B(S_0|R, z)$ many times. Consider the first crossing. Since S_0 and M_0 are equivalent variables, the trajectory can be thought of as representing a volume element of a Lagrangian volume V_0 that has Eulerian size R at z . Suppose the second crossing happened at M_1 (note that this requires $M_1 < M_0$). The same logic means that the trajectory could also have been thought of as representing a volume element of a Lagrangian volume V_1 that has Eulerian size R at z . We need to find a way of assigning a unique mass, a unique Lagrangian scale, to the trajectory.

If the various crossings of the barrier correspond to $M_0 > M_1 > \dots$, then the trajectory represents concentric Lagrangian regions $V_0 > V_1 > \dots$ that are now all within the same Eulerian region R at z . In effect, Bond et al. (1991) assume that successive concentric shells never cross; whereas the actual sizes of $V_0 > V_1 > \dots$ may change, the order of the shells is preserved. This means that if the largest region V_0 has Eulerian size V , then the subregions originally within it will remain within it. So the largest Lagrangian region associated with the trajectory, i.e., the one associated with the first crossing, is the one that should be associated with the trajectory. Counting the largest region V_0 at once includes all the smaller ones within it, and is the natural way to avoid double-counting the smaller regions.

Although Bond et al. (1991) considered only the case in which Lagrangian regions had collapsed to Eulerian size $R = 0$, their argument can also be applied in the $R > 0$ case studied here. Recall that, for a given z , curves for different R are nested (Fig. 2). Consider a trajectory $\delta_0(S_0)$ that crosses the barrier $B(R)$ for the first time at V_0 . The Lagrangian scale V_{n-1} , corresponding to the n th crossing of $B(R)$ by this same trajectory may be smaller than the Lagrangian scale V'_0 corresponding to the first crossing, by this trajectory, of the

barrier $B(R')$ for some Eulerian $R' \leq R$. In our model, such a trajectory represents a volume element of a Lagrangian region V_0 that at z , has Eulerian size R , at which time it contains a subregion that originally had size $V'_0 \leq V_0$ and now has size $R' \leq R$. The assumption is that if V'_0 has Eulerian size R' , and if $V_{n-1} < V'_0 \leq V_0$ originally, then all the mass M_{n-1} contained within V_{n-1} must still be contained within the Eulerian region R' now occupied by V'_0 . Thus the model developed here, in which the first crossing of a barrier $B(S_0|R, z)$ is used to assign a mass to a Lagrangian trajectory, explicitly preserves the ordering that was assumed by Bond et al.

Let $f(S_0, \delta_0|R, z) dS_0$ denote the fraction of trajectories that have their first crossing of the barrier between S_0 and $S_0 + dS_0$. Then, for a given barrier $B(S_0|R, z)$, $f(S_0, \delta_0|R, z) dS_0$ can be equated with the fraction of Lagrangian space that is associated with regions containing mass M_0 that each occupy an Eulerian region R at z . If $N(M_0|R, z) dM_0$ denotes the number of such regions, then each such region occupied a Lagrangian volume $V_0 = M_0/\bar{\rho}_0$, so

$$f(S_0, \delta_0|R, z) dS_0 = \frac{V_0 N(M_0|R, z) dM_0}{V_{\text{tot}}}, \quad (14)$$

where $V_{\text{tot}} \equiv \int V_0 N(M_0|R, z) dM_0$. Thus the distribution of first crossings gives an estimate of the number density of Lagrangian regions which contained mass M_0 and had initial over-density δ_0 , so that at z , while they still contain mass M_0 , they occupy the Eulerian volume V .

If we further suppose that the number of such regions is the same in both the Eulerian and Lagrangian spaces, then comparison with equation (1) shows that

$$p(M_0|R, z) dM_0 = \frac{V}{V_0} f(S_0, \delta_0|R, z) dS_0. \quad (15)$$

Since $(V_0/V) = M_0/(\bar{\rho}V) = (1 + \delta) = \Delta$, this means that

$$f(S_0, \delta_0|R, z) dS_0 = \Delta p(\Delta|R, z) d\Delta, \quad (16)$$

provided that δ_0 is the function of S_0 , R and z that is given by equation (10). This shows how the barrier-crossing distribution is related to $p(\Delta|R, z)$.

Notice that the left-hand side of equation (16) is determined by Lagrangian space quantities (the trajectories which cross the barrier are Lagrangian), whereas the right-hand side is associated with Eulerian space. A similar sort of relation between Lagrangian and Eulerian space quantities was used by Bernardeau (1994) (see the discussion at the start of his Section 3.2.2). The difference between his work and ours is that he used a Lagrangian distribution that was derived from perturbation theory, rather than from a barrier-crossing model, for the left-hand side of equation (16).

In summary, the Eulerian probability distribution function $p(M_0|R, z)$ is the fraction of regions of size R that, at z , contain mass M_0 . To estimate it, first assume that the initial fluctuation δ_0 is small, so $M_0/\bar{\rho}_0 = V_0 = (4\pi/3)R_0^3$. Next, choose a random position in the initial field. Compute δ_0 in spheres R_0 centred on this position. Call the curve $\delta_0(R_0)$ centred on this position a trajectory. Given R and z , draw the barrier $B(R_0|R, z)$ associated with the spherical collapse model (equation 10). The trajectory $\delta_0(R_0)$ may intersect the barrier $B(R_0|R, z)$ many times. Find the largest value of R_0 at which the trajectory intersects $B(R_0|R, z)$. Call this the first crossing of $B(R_0|R, z)$. Associate mass M_0 with this trajectory. Since mass M_0 and initial volume V_0 are equivalent, this trajectory represents a volume element of a region containing mass M_0 . Initially, M_0 had size $(4\pi/3)R_0^3$ and over-density $\delta_0(R_0|R, z)$. At z , it has size R . Repeat for an ensemble of such trajectories. So compute the distribution of first crossings of $B(R_0|R, z)$. The fraction of trajectories which first cross the barrier $B(R_0|R, z)$ at R_0 represents the fraction of mass that

is in regions of mass M_0 that, at z , have size R . From this, the average number density $N(M_0|R, z)/V_{\text{tot}}$ of such regions can be computed easily. Assume that the number of such regions is conserved. Then $N(M_0|R, z)V/V_{\text{tot}}$ equals $p(M_0|R, z)$.

2.4 The halo distribution

The previous subsection showed how to compute the Eulerian space distribution function using an excursion set model. However, the excursion set model can also be used to provide information about the halo distribution. This subsection shows why.

Following Bond et al. (1991), define a halo as a Lagrangian region that has collapsed to a vanishingly small Eulerian size: $R = 0$. Suppose z is given, and consider the Eulerian scale $R = 0$. In the spherical collapse model, $B(R_0|0, z)$ is independent of R_0 but depends on z (equation 10). Define $B(R_0|0, z) \equiv \delta_c(z)$. As before, equate the fraction of trajectories $f(R_0, \delta_c)$ which first cross $\delta_c(z)$ at R_0 with the fraction of mass in regions M_0 that, at z , have size $R = 0$. Following equation (14), the average number density of such regions is $\bar{n}(M_0, \delta_c) = N(M_0|0, z)/V_{\text{tot}} = (\bar{\rho}/M_0)f(R_0, \delta_c)$, and $\bar{n}(M_0|z)$ is said to be the mass function of collapsed haloes. This is exactly the excursion set model for the unconditional halo mass function developed by Bond et al. In the present context, the unconditional mass function is just the Eulerian distribution function in the limit $R = 0$.

Since the $R = 0$ limit has this special interpretation, in what follows, it is convenient to make a distinction between the barrier-crossing distribution in this limit, and that when $R > 0$. Below the subscript ‘c’ (for constant height), as in $f_c(S_0, \delta_0)$, denotes the barrier-crossing distribution when $R = 0$, and the subscript ‘R’ denotes the case $R > 0$.

Suppose we consider two-barriers $B_1 = B(S_0|R_1, z_1)$ and $B_0 = B(S_0|R_0, z_0)$, with $z_1 > z_0$. (It may help to look at Fig. 2.) For now, assume that $R_1 \leq R$. Let $f_R(S_1, \delta_1|S_0, \delta_0)$ denote the fraction of trajectories which first cross B_1 at S_1 given that they first crossed B_0 at S_0 . Again, consider the limit $R_1 = R = 0$ for both barriers. Then $B_1 = \delta_c(z_1) = \delta_{c1}$, and $B_0 = \delta_{c0}$ for all S_0 , so both barriers have a constant height, and $B_1 > B_0$. Bond et al. (1991) interpret $f_c(S_1, \delta_1|S_0, \delta_0)$ as representing the fraction of mass in an M_0 -halo that was earlier in M_1 -haloes. They define a conditional mass function as the average number of M_1 -haloes that are within an M_0 -halo: $\mathcal{N}(1|0) = (M_0/M_1)f_c(1|0)$ if $M_1 \leq M_0$, and $\mathcal{N}(1|0) = 0$ otherwise. In the context of this paper, $f_c(1|0)$ represents the fraction of the Lagrangian region V_0 that has Eulerian size $R = 0$ at z_0 , which was previously in Lagrangian regions V_1 that, at z_1 , also occupied vanishingly small Eulerian volumes. The reason for wording things in this way is that it shows how to compute other properties of the halo distribution in Eulerian space.

For example, the average number of M_1 haloes that collapsed at z_1 and are in Eulerian regions $R > 0$ at $z < z_1$ can be computed as follows. Recall that (M_1, z_1) -haloes are associated with trajectories which cross the constant barrier $B_1 = \delta_{c1}$ at S_1 . Since $\delta_{c1} > \delta_c(z)$, and since B_0 decreases monotonically as S_0 increases, each of these trajectories must have crossed $B_0 = B(S_0|R, z)$ at some $S_0 \leq S_1$, so as to reach $\delta_c(z_1)$ at S_1 . Therefore

$$f_c(S_1, \delta_{c1}) = \int_0^{S_1} f_c(S_1, \delta_{c1}|S_0, \delta_0) f_R(S_0, \delta_0) dS_0, \quad (17)$$

where $\delta_0 = B(S_0|R, z)$. Since $f_c(1) = (M_1/\bar{\rho})\bar{n}(1)$, $f_c(1|0) = (M_1/M_0)\mathcal{N}(1|0)$, $f_R(0) dS_0 = \Delta p(\Delta) d\Delta$, and $\Delta = M_0/\bar{\rho}V$,

equation (17) implies that

$$\bar{n}(M_1, \delta_{c1})V = \int_0^\infty \mathcal{N}(M_1, \delta_{c1}|M_0, \delta_0) p(M_0|R, z) dM_0. \quad (18)$$

If we set

$$N(1|0) = \mathcal{N}(M_1, \delta_{c1}|M_0, \delta_0), \quad (19)$$

where $N(1|0)$ was defined in Section 2, just prior to equation (5), and δ_0 in $\mathcal{N}(1|0)$ is given by equation (10), and we recall that $p(M_0) dM_0 = p(\Delta) d\Delta$ (equation 3), then this expression is the same as equation (5). Equation (19) shows that the average number of M_1 -haloes in Eulerian cells V which contain mass M_0 at z is equal to that in those Lagrangian regions V_0 which had initial density δ_0 given by equation (10).

The main reason for writing this out explicitly is that it shows how statistics in the Lagrangian space can be used to compute statistics in Eulerian cells V . Namely, the assumed conservation of number of regions in the two spaces (equation 18 equals equation 5) means that an average over Eulerian regions of size V is equivalent to averaging over those Lagrangian regions that have evolved into Eulerian regions of size V (equations 18 and 19). In practice, this means that Eulerian space quantities like $\bar{\xi}_{\text{hm}}$ and $\bar{\xi}_{\text{hh}}$ can be computed simply by using the appropriate value for δ_0 (that given by equation 10) in the associated Lagrangian space quantities, and then summing over M_0 , weighting the contribution from each M_0 appropriately. This weighting is given by the barrier-crossing algorithm, because the barrier-crossing distribution $f_R(S_0, \delta_0)$, with δ_0 given by equation (10), represents the fraction of Lagrangian space that is associated with regions of mass M_0 that, because they had initial over-density δ_0 , are Eulerian regions of size V at z .

Section 3 illustrates how this works. It presents a model in which all these quantities can be computed analytically.

2.5 Relation to the work of Mo & White

Before moving on, it is interesting to compare this model with previous work. Our equation (19) is exactly the same as that assumed by Mo & White (1996). They assumed that the Eulerian space quantity $N(1|0)$ could be computed by simply substituting the spherical collapse value of $\delta_0(R_0|R, z)$ into the Lagrangian formula $\mathcal{N}(1|0)$. They showed that the resulting formula for $N(1|0)$ provided good fits to the corresponding Eulerian space quantity measured in their numerical simulations of clustering. Since, in this regard, our model leads to the same formula as that of Mo & White, the agreement with simulations provides some justification for the strong simplifying assumptions which lead to our model.

Our model extends their results in the following way. Our equation (18) shows that, to compute averages in Eulerian space, knowledge of the Eulerian space distribution function $p(\Delta|R, z)$ is necessary to then take the correct average over Lagrangian regions V_0 that have become Eulerian regions V . Mo & White also knew this, but they did not know how to compute $p(\Delta|R, z)$. They therefore assumed that it could be taken directly from their numerical simulations. However, as our approach shows, $p(\Delta|R, z)$ is related to the shape of the boundary (cf. our equation 16). This relation must not be ignored. To see why, suppose (as Mo & White did) that a lognormal can be substituted for $p(\Delta|R, z)$. If one uses the spherical model for $\delta_0(R_0|R, z)$ in $\mathcal{N}(1|0)$ and then does the integral on the right-hand side of (18), one finds that it does not equal the correct value for the left-hand side. This is because, as our approach shows, self-consistency requires that $p(\Delta|R, z)$ depend on the boundary shape; once the boundary is specified, one is no longer free to

choose any arbitrary distribution for $p(\Delta|R, z)$. This may partially explain why the Mo & White results using a lognormal are somewhat worse than when they use the distribution measured directly in their simulations.

Since our approach shows how to derive $p(\Delta|R, z)$ from the boundary shape, our approach can be thought of as deriving, self-consistently, the Mo & White (1996) spherical evolution formulae by a simple extension of the Bond et al. (1991) excursion set approach.

2.6 The two-barrier problem

The previous subsection showed that problems involving the crossing of two-barriers, in which one barrier was assumed to be constant, and the other not (i.e., the Eulerian scale was $R = 0$ for one barrier, but $R > 0$ for the other), could be used to provide information about the distribution of haloes within Eulerian cells V . The case in which $R > 0$ for both barriers is also interesting.

Consider two-barriers $B(R_0|R, Z)$ and $b(r_0|r, z)$. If $z = Z$ and $r < R$, then the two-barrier problem is associated with the joint distribution of the mass within two concentric Eulerian cells. It may therefore be useful for estimating the evolved Eulerian space density profile. Of course, in the model, haloes collapse to zero radius, and this is unrealistic. In practice, haloes virialize at some fraction of their turnaround radius. Therefore the solution of this two-barrier problem is probably only useful on scales larger than the virial radius.

If, instead, $r = R$, but $z > Z$, then the two-barrier problem describes the matter within the same comoving cell at two different epochs. That is, it can be used to quantify the way in which matter flows in and out of (comoving) Eulerian cells.

3 THE LINEAR BARRIER AND WHITE-NOISE INITIAL CONDITIONS

This section shows how the model described in Section 2 can be used. It assumes that the initial Lagrangian space distribution is white-noise Gaussian and studies the first-crossing distribution of a barrier whose height decreases linearly as $V_0 = (4\pi/3)R_0^3$ decreases:

$$B(S_0|R, z) = \delta_{c0} (1+z) - \frac{\delta_{c0} (1+z)}{\Delta}, \quad (20)$$

where $S_0 = 1/\bar{\rho}_0 V_0$, and $\Delta = M_0/\bar{\rho}V = (R_0/R)^3$.

This barrier shape was chosen for a number of reasons. First, this shape is a simple approximation to the spherical collapse barrier (compare equation 10, and see Fig. 2), and the associated dynamical evolution is similar. Section 3.1 shows how the evolution of a spherical perturbation in this model differs from that in the usual spherical collapse model. Second, the first-crossing distribution of a linear barrier is known, so the associated Eulerian distribution can be written analytically; it is Inverse Gaussian. The Inverse Gaussian is a good approximation to the distribution measured in numerical simulations of clustering from white-noise initial conditions (Section 3.6), so the model may also be realistic. Finally, for this barrier, the halo–mass and halo–halo correlations can all be computed analytically.

3.1 Relation to the spherical collapse model

The linear barrier studied in this section is associated with the following model for the collapse of objects.

Let $R(z)$ denote the comoving size of an object at the epoch z . Then $R(z) = R_0$ initially. If the object is in an underdense region, then its comoving size will increase, else it will decrease. Trajectories with extrapolated linear over-density δ_0 greater than δ_{c0} are associated with collapsed objects. Collapsed objects have $R(z) = 0$. Equation (20) implies that, before collapse,

$$\frac{R^3(z)}{R_0^3} = 1 - \frac{\delta_0(1+z)}{\delta_{c0}}. \quad (21)$$

The radius of an object in proper, physical coordinates is $R_p(z) = R(z)(1+z)$. Objects which collapse have a turnaround radius – the maximum value that $R_p(z)$ attains. This occurs at

$$(1+z_{ta}) = \frac{4\delta_0}{3\delta_{c0}}, \quad (22)$$

at which time

$$\frac{R(z_{ta})}{R_0} = \frac{1}{4^{1/3}}. \quad (23)$$

In comparison, collapsing objects in the spherical model reach turnaround at

$$(1+z_{ta}) = 4^{1/3} \frac{\delta_0}{\delta_{c0}}, \quad (24)$$

at which time

$$\frac{R(z_{ta})}{R_0} = \frac{(1+z_{ta})R_p(z_{ta})}{R_0} = \frac{6}{10} \frac{4^{1/3}}{\delta_{c0}} = \left(\frac{4}{3\pi}\right)^{2/3} \quad (25)$$

(e.g. Peebles 1980). Fig. 3 shows that, for over-dense perturbations, turnaround in this model (dashed lines) occurs later, and at a larger radius, than in the spherical model (solid lines). To compensate, underdense regions expand less rapidly in this model than in the spherical model.

3.2 The constant barrier and statistics in Lagrangian space

In the limit $R \rightarrow 0$, equation (20) for the barrier shape becomes independent of S_0 , as it does for the spherical collapse model. In this limit, the first-crossing distribution is known (e.g. Bond et al. 1991),

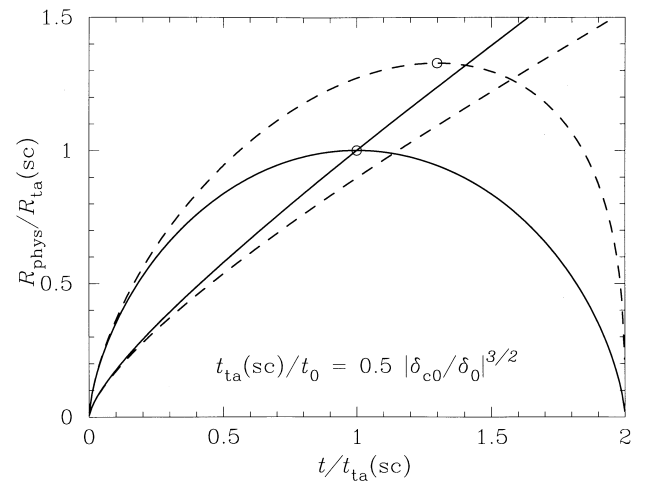


Figure 3. The physical radius of a perturbation in units of the spherical model turnaround radius, as a function of time in units of the spherical collapse model turnaround time. The solid curves show the spherical model, and the dashed curves show the linear barrier model studied in this paper. The two curves for each line type are for denser perturbations (which recollapse) and underdense perturbations (which do not).

although we give a different derivation of it below. Therefore, to set notation, this section summarizes various known results about the crossing of a constant barrier by the Lagrangian trajectories described earlier, under the assumption that $\delta_0(\mathbf{r}; 0)$ is a Gaussian random field.

Let $p(S_0, \delta_0) d\delta_0$ denote the fraction of trajectories that have value between δ_0 and $\delta_0 + d\delta_0$ at S_0 . Also, let $p(S_0, \delta_0|S', \delta', \text{first}) d\delta_0$ denote the fraction of those trajectories which first crossed the barrier $B(S_0|R, z)$ between S' and $S' + dS'$, which have values between δ_0 and $\delta_0 + d\delta_0$ at $S_0 \geq S'$. Then

$$p(S_0, \delta_0) = \int_0^{S_0} p(S_0, \delta_0|S', \delta', \text{first}) f(S', \delta'|R, z) dS', \quad (26)$$

provided that at S_0 , $\delta_0 \geq B(S_0|R, z)$. If both $p(S_0, \delta_0)$ and $p(S_0, \delta_0|S', \delta', \text{first})$ are known, then this is a Volterra equation of the first kind, so it can be solved numerically, by forward substitution, to yield $f(S', \delta'|R, z)$.

Suppose that the probability distribution of the density in the Lagrangian space is Gaussian. Then

$$p(S_0, \delta_0) d\delta_0 = \frac{d\delta_0}{\sqrt{2\pi S_0}} \exp\left(-\frac{\delta_0^2}{2S_0}\right). \quad (27)$$

If the window W is sharp in k -space, then

$$p(S_0, \delta_0|S', \delta', \text{first}) d\delta_0 = p(S_0, \delta_0|S', \delta') d\delta_0, \quad (28)$$

and

$$p(S_0, \delta_0|S', \delta') d\delta_0 = \frac{d\delta_0}{\sqrt{2\pi(S_0 - S')}} \exp\left[-\frac{(\delta_0 - \delta')^2}{2(S_0 - S')}\right] \quad (29)$$

(e.g. Bond et al. 1991). Thus, if the Lagrangian space distribution is Gaussian, and the window function is sharp in k -space, then the distribution of first-crossing times is easy to compute, whatever the boundary shape. Equations (28) and (29) are also correct for a top-hat filter in real space, if the Gaussian field is white noise. So the distribution of first-crossing times is easy to compute for white noise also. In either of these cases, a trajectory $\delta_0(S_0)$ resembles the motion of a particle undergoing standard Brownian motion with zero drift. Bond et al. (1991) and Lacey & Cole (1993) used this fact to compute $f(S_0, \delta_0)$.

Notice, however, that when the boundary is a constant, $B(S_0|R = 0, z) = \delta_{c0}(1 + z) \equiv \delta_c(z)$, then the form of $f(S_0, \delta_0)$ can be obtained directly from equation (26). First, take the derivative with respect to δ_0 on both sides of equation (26), and evaluate it at $\delta_0 = \delta_c(z)$. Next, set $\delta' = \delta_c(z)$. Then the integrand on the right-hand side is zero, except when $S' = S_0$. Thus equation (26) implies that

$$\begin{aligned} f_c(S_0, \delta_c[z]) &= \frac{\delta_c(z)}{S_0} p[S_0, \delta_c(z)] \\ &= \frac{\delta_c(z)}{\sqrt{2\pi S_0}} \exp\left[-\frac{\delta_c^2(z)}{2S_0}\right] \frac{dS_0}{S_0}, \end{aligned} \quad (30)$$

where the subscript 'c' denotes the fact that this is the distribution of first crossings of a constant boundary.

If the trajectory is known to start from (S_0, δ_{c0}) , rather than from the origin, then the distribution of first crossings of the constant barrier $\delta_{c1} = \delta_{c0}(1 + z_1)$ can be solved similarly. Provided $\delta_{c1} > \delta_{c0}$ and $S_1 > S_0$,

$$f_c(S_1, \delta_{c1}|S_0, \delta_{c0}) = \left(\frac{\delta_{c1} - \delta_{c0}}{S_1 - S_0}\right) p(S_1, \delta_{c1}|S_0, \delta_{c0}). \quad (31)$$

These expressions for the first-crossing distribution are the same as those derived by Bond et al. (1991) and Lacey & Cole (1993).

Following Bond et al. (1991), treat the parameter $\delta_c(z)$ as a pseudo-time variable; it decreases as the Universe evolves. Then associate the first-crossing distribution of the barrier $\delta_c(z)$ with a number density of regions containing mass M_0 in the Lagrangian space, and call every such region a dark matter halo. Then the number density of M_1 haloes at the epoch labelled by $\delta_{c1} = \delta_c(z_1)$ is

$$\bar{n}(M_1, \delta_{c1}) dM_1 \equiv \frac{\bar{\rho}_0}{M_1} f_c(S_1, \delta_{c1}) dS_1. \quad (32)$$

This is consistent with equation (14), and $\bar{n}(M_1, \delta_{c1})$ is sometimes called the unconstrained halo mass function at the epoch z_1 .

Similarly, the average number of (M_1, δ_{c1}) -haloes that are within an (M_0, δ_{c0}) -halo is

$$\mathcal{N}(1|0) \equiv \left(\frac{M_0}{M_1}\right) f_c(S_1, \delta_{c1}|S_0, \delta_{c0}) \frac{dS_1}{dM_1} \quad (33)$$

(e.g. Lacey & Cole 1993). This is the constrained mass function.

The joint distribution of the number N_1 of (M_1, δ_{c1}) -haloes and the number N_2 of (M_2, δ_{c2}) -haloes, that are both within the same (M_0, δ_{c0}) -halo, averaged over all (M_0, δ_{c0}) -haloes is

$$C(12|0) \equiv \langle N_1 N_2, \delta_{c1} | M_0, \delta_{c0} \rangle = \mathcal{N}(1|0) \mathcal{N}(2|10), \quad (34)$$

where $\mathcal{N}(1|0)$ is given by equation (33), and

$$\mathcal{N}(2|10) dM_2 = \frac{M_0 - M_1}{M_2} f_c(S_2, \delta_{c2}|S_{01}, \delta_{01}) dS_2 \quad (35)$$

(Sheth 1996b). Here $S_{01} = S(M_0 - M_1) = (M_0 - M_1)^{-1}$, and δ_{01} is the over-density in the remaining volume $V_0 - V_1$ that is not occupied by the M_1 -halo. That is,

$$1 + \delta_{01} = \frac{M_0 - M_1}{\bar{\rho}_0(V_0 - V_1)}. \quad (36)$$

However, $M_0 \equiv \bar{\rho}_0 V_0(1 + \delta_{c0})$ and $M_1 \equiv \bar{\rho}_0 V_1(1 + \delta_{c1})$, so that, to lowest order,

$$\begin{aligned} \delta_{c1} - \delta_{01} &= (\delta_{c1} - \delta_{c0}) \frac{M_0(1 + \delta_{c1})}{M_0(1 + \delta_{c1}) - M_1(1 + \delta_{c0})} \\ &\approx (\delta_{c1} - \delta_{c0}) \frac{M_0}{M_0 - M_1}. \end{aligned} \quad (37)$$

Most of the formulae in this section are not new, but they will all be useful below. They have been included to set notation, and because, as the previous section showed, if these expressions are known, then simple transformations allow one to compute the associated Eulerian space quantities.

3.3 The linear barrier-crossing distribution and the matter distribution in Eulerian space

The previous subsection described the first-crossing distribution associated with a constant barrier by trajectories associated with a Lagrangian field that is Gaussian white noise. Recall that the constant barrier is got from the linear barrier of equation (20) by setting $R = 0$. When $R > 0$, then direct substitution shows that

$$f_R(S_0, \delta_0) dS_0 = \frac{B(0|R, z)}{\sqrt{2\pi S_0}} \exp\left(-\frac{B^2(S_0|R, z)}{2S_0}\right) \frac{dS_0}{S_0}, \quad (38)$$

where B is given by equation (20), satisfies equation (26). The identity

$$\int_0^\infty f_R(S_0, \delta_0) dS_0 = 1, \quad (39)$$

which follows from the definition of the modified Bessel function of the third kind, is useful in proving this result. A full derivation of this distribution is given in Appendix A.

Equation (38) is known as the Inverse Gaussian distribution. It was first discovered in the context of Brownian motion by Schrödinger (1915). Folks & Chhikara (1978) give a review of its role in other fields. Here, the distribution represents the fraction of Lagrangian space which is associated with regions of mass $M_0(S_0)$ provided the initial distribution is white-noise Gaussian, and the dynamics are a simple modification of the usual spherical collapse model (as described in the previous subsection.)

For white noise, $M_0 = 1/S_0$, so, for white noise, equation (38) in (16) implies that the Eulerian distribution function that is associated with the linear barrier is

$$p(\Delta|R) d\Delta = \bar{\rho} V S_0 f_R(S_0, \delta_0) dS_0 \\ = \frac{1}{\sqrt{2\pi\bar{\xi}_m\Delta}} \exp\left[-\frac{(\Delta - \mu)^2}{2\bar{\xi}_m\Delta}\right] \frac{d\Delta}{\Delta}, \quad (40)$$

where

$$\bar{\xi}_m(R) \equiv [\delta_{c0}^2(1+z)^2\bar{\rho}V]^{-1}, \quad \text{and } \mu = 1, \quad (41)$$

and we have not bothered to write the z dependence of $p(\Delta|R, z)$ explicitly. Notice that $p(\Delta|R)$ is also an Inverse Gaussian distribution. The mean of this distribution is $\mu = 1$, and the variance is $\bar{\xi}_m$. The higher order moments of this distribution are simple. If $\bar{\xi}_n$ is the n th cumulant of this distribution, then

$$S_n \equiv \frac{\bar{\xi}_n}{\bar{\xi}_m^{n-1}} = (2n - 3)!! \quad (42)$$

and it is independent of cell size V . This is simply a consequence of the fact that, in the model, haloes have vanishingly small Eulerian sizes: $R = 0$.

As $\bar{\xi}_m \rightarrow 0$, this Inverse Gaussian tends to the Gaussian distribution. For fixed V , this happens if $\delta_{c0}(1+z) \gg 1$. Since z is a pseudo-time variable, this means that, at sufficiently early times, the Eulerian distribution is Gaussian for almost all scales V . This is sensible, since at early times the Eulerian and Lagrangian distributions should be similar, and, by hypothesis, the Lagrangian distribution is Gaussian. For a given z , $\bar{\xi}_m \rightarrow 0$ as $V \gg 1$. This means that, even at later times, the Eulerian distribution function, measured in sufficiently large cells V , appears Gaussian.

When $V \rightarrow 0$, then the term in the exponent of equation (40) tends to $\Delta/\bar{\xi}_m = \delta_{c0}^2(1+z)^2/S_0$, so $p(\Delta|R) \rightarrow V$ times equation (32), which is the same as $1/\Delta$ times equation (30). This is consistent with the fact that, in this limit, equation (20) shows that the barrier shape tends to the constant $\delta_{c0}(1+z)$, and the first-crossing distribution of a constant barrier is given by equation (30). This shows explicitly that the unconstrained mass function of (32) is essentially the same as the Eulerian distribution function, in the limit of vanishing cell size V . All these asymptotic relations are sensible.

3.4 The halo distribution

A little algebra shows that when the barrier shape is linear, then equation (17) is satisfied for all R . Recall that that expression simply expresses the fact that the fraction of trajectories which first cross the constant barrier δ_{c1} at S_1 is equal to the fraction of trajectories which first cross the linear barrier (associated with the Eulerian scale R) at $\delta_0 = B(S_0|R, z_0)$, and then cross the constant barrier $\delta_{c1} \geq \delta_{c0}$ at S_1 , summed over all $S_0 \leq S_1$. Of course, this implies that equation (18) is also satisfied: $\bar{n}(M_1, \delta_{c1})V$ is equal to V times equation (32), as it should. This shows explicitly that, for the linear barrier, the number density of haloes in the Eulerian space is equal to that in the Lagrangian space, and this number density is just what is required by the Bond et al. (1991) excursion set approach.

The cross-correlation between haloes and mass can be worked out similarly. Start with equation (7). Use equation (16) to write $p(\Delta|R, z_{\text{obs}})$ in terms of the Lagrangian barrier-crossing distribution $f_R(S_0, \delta_0)$. Then use (38) for $f_R(S_0, \delta_0)$, and recall that $\delta_0 = B(S_0|R, z_{\text{obs}})$ where equation (20) gives B . This means that $B(0|R, z) = \delta_{c0}(1+z_{\text{obs}})$, where $z_{\text{obs}} \leq z_1$. Then use equation (19) to set $N(1|0) = \mathcal{N}(1|0)$, and use (33) for $\mathcal{N}(1|0)$ with $\delta_0 = B(S_0|R, z_{\text{obs}})$. With these substitutions, the integral in equation (7) can be solved analytically:

$$\bar{\xi}_{\text{hm}}(1|R) = \frac{M_1}{\bar{\rho}V} \left(\frac{1+z_1}{1+z_{\text{obs}}} \right) + \frac{M_*(z_{\text{obs}})}{\bar{\rho}V} \left(\frac{z_1 - z_{\text{obs}}}{1+z_1} \right), \quad (43)$$

where

$$\delta_{c1} = \delta_{c0}(1+z_1), \quad \delta_{c0}^2/S_0 = M_0/M_{*0}, \quad \text{and} \\ M_*(z_{\text{obs}}) = M_{*0}(1+z_{\text{obs}})^{-2}. \quad (44)$$

Notice that when $z_1 = z_{\text{obs}}$, then $\bar{\xi}_{\text{hm}} = M_1/\bar{\rho}V$. That is, the only correlation that arises is that which is due to the fact that there is a halo of mass M_1 inside V , so there is certainly mass M_1 inside V . Since

$$\bar{\xi}_m(R) = \frac{1}{\delta_{c0}^2(1+z_{\text{obs}})^2\bar{\rho}V} = \frac{M_*(z_{\text{obs}})}{\bar{\rho}V},$$

equations (41) and (44) imply that

$$\frac{\bar{\xi}_{\text{hm}}(1|R)}{\bar{\xi}_m(R)} = \frac{M_1}{M_*(z_{\text{obs}})} \left(\frac{1+z_1}{1+z_{\text{obs}}} \right) + \left(\frac{z_1 - z_{\text{obs}}}{1+z_1} \right). \quad (45)$$

This ratio is independent of the Eulerian cell size V . Again, this a consequence of the fact that the model assumes that haloes have zero volume, so if a halo is within a cell, then all its associated mass is also.

This expression has an interesting relation to previous work. Mo & White (1996) argue that, when $|\delta_{c0}| \ll \delta_{c1}$, then, in the limit of large V ,

$$\langle \delta_{\text{h}}(1|0) \delta \rangle_{\text{R}} \approx \left\{ 1 + \frac{(\nu_1^2 - 1)/\delta_{c0}}{\delta_{c1}/[\delta_{c0}(1+z_{\text{obs}})]} \right\} \langle \delta^2 \rangle, \quad (46)$$

where $\nu_1^2 \equiv \delta_{c1}^2/S_1$. Now, $\delta_{c1}/\delta_{c0} = (1+z_1)$, and $\langle \delta^2 \rangle \approx \bar{\xi}_m$ for large V , so this expression is the same as what is required by equations (44) and (45) if $\delta_{c0} = 1$. The extra factor of δ_{c0} arises from the fact that, for large V , the density fluctuation δ in most Eulerian cells is small, so $\Delta \equiv 1 + \delta \approx 1$ for most V . In this limit, equation (10) shows that $\delta_0/(1+z) \approx \delta$ in the collapse spherical model, whereas equation (20) shows that it is $\approx \delta_{c0}\delta$ for the linear barrier.

Let $\bar{\xi}_{\text{hh}}(M_1, M_2, \delta_{c1}|R)$ denote the correlation function of M_1 and M_2 haloes identified at the epoch z_1 , averaged over all comoving Eulerian cells V , at the epoch $z_{\text{obs}} \leq z_1$. Recall that this average can be computed in two steps. All Eulerian cells can be classified by the mass M_0 within them. Further classify all Eulerian cells which contain mass M_0 by their Lagrangian over-density δ_0 . Since the number of such regions is conserved, the joint distribution of the number of M_1 and M_2 haloes, $N_1 N_2$, averaged over all such (M_0, δ_0) -regions, is the same in both spaces, provided we set $\delta_0 = B(S_0|R, z)$. This average gives $C(12|0)$ of equation (34), where $\delta_0 = B(S_0|R, z)$ and B is given by (20). All that remains is to further average $C(12|0)$ over the number of such conserved regions. This is done by weighting it by $p(\Delta|R)$, integrating over Δ , and then dividing out the factors expected on average. We have gone to the trouble of stating things this way to show that our definition of $\bar{\xi}_{\text{hh}}(12|R)$ includes the effects of the scatter of halo counts in Eulerian regions which had the same over-density as well as the same radius initially.

Therefore, $\bar{\xi}_{\text{hh}}$ here denotes the same quantity as σ_{hh}^2 of equation (25) in Mo & White (1996).

Now, $1 + \bar{\xi}_{\text{hh}}(12|R)$ is given by equation (8), where $C(12|0)$ is given by equation (34). With equations (16) and (38) for $p(\Delta|R)$, and setting $\delta_0 = B(S_0|R, z)$ as before, this integral can be solved analytically. The result is that

$$\frac{\bar{\xi}_{\text{hh}}(12|R)}{\bar{\xi}_{\text{m}}(R)} = \frac{M_1 + M_2}{M_*(z_{\text{obs}})} \left(\frac{z_1 - z_{\text{obs}}}{1 + z_{\text{obs}}} \right) + \left(\frac{z_1 - z_{\text{obs}}}{1 + z_1} \right)^2, \quad (47)$$

where $z_1 \geq z_{\text{obs}}$, and $M_*(z_{\text{obs}})$ is defined as before. Like the halo–mass correlation function, this ratio is independent of V because, in the model, haloes are point-sized. Thus, in the model, haloes are linearly biased tracers of the mass on all scales. Mo & White (1996) argue that $\bar{\xi}_{\text{hh}}/\bar{\xi}_{\text{m}}$ should equal $(\bar{\xi}_{\text{hh}}/\bar{\xi}_{\text{m}})^2$ on large scales. Although our equation (45) for $\bar{\xi}_{\text{hh}}/\bar{\xi}_{\text{m}}$ is similar to theirs, the right-hand side of our equation (47) is not the same as the square of the right-hand side of equation (45); they differ by a factor of $[M(1 + z_1)/M_*(z_{\text{obs}})(1 + z_{\text{obs}})]^2$.

When $z_1 = z_{\text{obs}}$, $\bar{\xi}_{\text{hh}}(12|R) = 0$, which implies that haloes, when they first virialize, are uncorrelated with each other. Further, the correlation of haloes depends on the sum of the halo masses, but not on the masses themselves. This suggests that halo–halo correlations arise because of volume exclusion effects only. That is, halo–halo correlations arise from the fact that an M_1 -halo occupies a region V_1 initially, so no other halo can occupy this region. The correlation function is affected by the fact that a region is included, but not by the exact way in which the excluded region is populated.

If the halo masses M_1 and M_2 and their formation epoch z_1 are fixed, then the halo–halo correlation function at a given comoving R increases as z_{obs} decreases. This increase reflects the fact that haloes which formed at z_1 , at which time they were uncorrelated with each other, must have merged with each other to construct the more massive haloes present at the later epoch $z_{\text{obs}} \leq z_1$. Suppose, instead, that the halo masses, the comoving scale, and the epoch at which the halo distribution is measured (i.e., z_{obs}), are given, and we wish to consider the effect of changing the halo formation epoch $z_1 \geq z_{\text{obs}}$. Equation (47) shows that as z_1 decreases to z_{obs} , $\bar{\xi}_{\text{hh}}$ decreases. That is, at fixed mass, the halo–halo correlation function in comoving coordinates exhibits negative evolution.

3.5 The two-barrier problem

The previous subsections showed how the first crossing of a linear barrier by Brownian walks could be used to compute various interesting quantities associated with gravitational clustering. This section shows that the associated two-barrier problem may also be useful. In general, the linear barrier has two free parameters which may be thought of as the y -intercept δ_{c0} and the slope β , respectively:

$$\delta_0(S_0) = \delta_{c0} - \beta S_0. \quad (48)$$

Below, we consider the statistics of trajectories which first cross a barrier with one choice of parameters, and then cross another.

First, consider two-barriers δ_1 and δ_2 which have the same y -intercept δ_{c0} , but different slopes, β_1 and β_2 . Assume that $\beta_2 > \beta_1$. This means that trajectories must cross the barrier δ_2 before they can cross δ_1 . We seek an expression for the probability that a trajectory has its first crossing of δ_1 at S_1 , given that it has its first crossing of the barrier δ_2 at $S_2 \leq S_1$. Recall the derivation of the barrier-crossing distribution given in Appendix A. To a particle that started from the origin and has just crossed the barrier $\delta_2(S_2)$, the barrier

$\delta_1(S_1)$ has shape

$$\begin{aligned} \delta_{12}(S_1 - S_2) &= \delta_1(S_1) - \delta_2(S_2) \\ &= (\beta_2 - \beta_1)S_2 - \beta_1(S_1 - S_2) \end{aligned} \quad (49)$$

Since this barrier is also linear, the solution is the same as before, except that $S_0 \rightarrow S_1 - S_2$ and $\delta_c \rightarrow \delta_{12}$. Therefore the first-crossing distribution is

$$f(S_1, \delta_1|S_2, \delta_2) dS_1 = \frac{(\beta_2 - \beta_1)S_2}{\sqrt{2\pi(S_1 - S_2)}} \exp\left[-\frac{(\beta_2 S_2 - \beta_1 S_1)^2}{2(S_1 - S_2)}\right] \frac{dS_1}{(S_1 - S_2)}. \quad (50)$$

Since δ_{c0} is a pseudo-time variable, and it is the same for the two-barriers, equation (48) shows that the expression above will be useful for computing statistics in concentric cells V_1 and $V_2 > V_1$, at the same epoch. Therefore it may be useful for computing Eulerian density profiles within the context of the model. Since, in the model, haloes collapse to zero radius, this way of computing density profiles is probably only useful on scales larger than the virial radius. The virial radius can be derived from combining the spherical collapse model with the fact that the mass within the virial radius is given by the scale at which the trajectory first crosses δ_{c0} .

The corresponding expression for two-barriers which have the same slope β , but have different values for the y -intercept, say, δ_{c1} and $\delta_{c2} < \delta_{c1}$, is

$$\begin{aligned} f(S_1, \delta_1|S_2, \delta_2) dS_1 &= \frac{(\delta_{c1} - \delta_{c2})}{\sqrt{2\pi(S_1 - S_2)}} \\ &\times \exp\left\{-\frac{[(\delta_{c1} - \delta_{c2}) - \beta(S_1 - S_2)]^2}{2(S_1 - S_2)}\right\} \frac{dS_1}{(S_1 - S_2)}. \end{aligned} \quad (51)$$

Equation (48) shows that this provides information about the matter in concentric cells V_1 and $V_2 > V_1$, at two different epochs. Since the value of β is the same, the two cell sizes are related: $(V_2/V_1) = (\delta_{c1}/\delta_{c2})$.

More interesting, perhaps, is the case in which the cell sizes V are the same, but $\delta_{c1} > \delta_{c2}$. This case is also more complicated, since now it is possible to cross barrier 1 before crossing barrier 2. Provided $S_2 < \bar{\rho}V$,

$$\begin{aligned} f(S_1, \delta_1|S_2, \delta_2) dS_1 &= \frac{\delta_{c12}}{\sqrt{2\pi(S_1 - S_2)}} \\ &\times \exp\left\{-\frac{[\delta_{c12} - \beta_1(S_1 - S_2)]^2}{2(S_1 - S_2)}\right\} \frac{dS_1}{(S_1 - S_2)}, \end{aligned} \quad (52)$$

where $\delta_{c12} = (\delta_{c1} - \delta_{c2})(1 - \beta_2)$, and β_1 and β_2 are given by using (20) in (48), with δ_{c1} and δ_{c2} , respectively. When the first crossing of δ_2 occurs at $S_2 > \bar{\rho}V$, then the trajectory will have crossed δ_1 first. In this case, $f(S_2, \delta_2|S_1, \delta_1)$, with $S_2 \geq S_1$, is given by the expression above, provided the labels 1 and 2 are interchanged. These expressions contain information about the mass in the same comoving Eulerian cell at different epochs. They show that it is possible that the mass in V first decreases and later increases. This shows explicitly that, in the model, matter can flow in and out of Eulerian cells.

3.6 Comparison with simulations

This subsection shows that the Inverse Gaussian distribution provides a good description of the evolved distribution for clustering from white-noise initial conditions. Before doing so,

we first argue that such a test has, in fact, already been performed by others.

The Inverse Gaussian is a limiting form of the generalized Poisson distribution (GPD)

$$p(N|R, b) = \frac{\bar{N}_c}{N!} (\bar{N}_c + Nb)^{N-1} e^{-\bar{N}_c - Nb}, \quad (53)$$

where N is the number of identical particles in a randomly placed cell of size R which contains \bar{N} particles on average, $\bar{N}_c \equiv \bar{N}(1 - b)$, and $0 \leq b \leq 1$. In the astrophysical context, the GPD was first derived by Saslaw & Hamilton (1984). It can be related to the Inverse Gaussian as follows (Fry 1985; Sheth 1996a). The mean of this discrete distribution is \bar{N} , and the variance is $\bar{N}/(1 - b)^2 \equiv \bar{N}(1 + \bar{N}\bar{\xi})$. Notice that as $\bar{N} \rightarrow \infty$ and $b \equiv (1 + \delta_{c0})^{-1} \rightarrow 1$, $\bar{N}\bar{\xi} \rightarrow \delta_{c0}^{-2}$, which is the relation required by equation (41). In this limit, $\bar{N}p(N|R, b)$ tends to the Inverse Gaussian distribution $p(\Delta|R)$, since $N/\bar{N} \equiv \Delta$.

Sheth (1998) shows that the GPD can be derived using a boundary crossing, excursion set model associated with the Poisson distribution in the initial Lagrangian space. The linear barrier shape considered in this paper is a limiting form of that associated with the Poisson case. This correspondence is important, since the GPD is in good agreement with numerical simulations of clustering from Poisson initial conditions (Itoh, Inagaki & Saslaw 1993, and references therein), provided the variance is allowed to be a free function of scale. Bouchet & Hernquist (1992) showed that the GPD also describes clustering from white-noise initial conditions well. This just reflects the (intuitively obvious) fact that clustering from Poisson and white-noise initial conditions should evolve similarly. Since the Inverse Gaussian is just a limiting form of the GPD (just as the white-noise Gaussian is a limiting form of the Poisson distribution), the Inverse Gaussian should provide a good approximation to the Eulerian distribution measured in simulations of clustering from white-noise initial conditions, in the regime where discreteness effects are unimportant. Fig. 4 shows this explicitly.

The simulations of clustering from white-noise initial conditions used here are the same as those studied by Mo & White (1996), where they are described in more detail. The simulations contain 10^6 particles in a cube with periodic boundary conditions. Fig. 4 shows the evolved Eulerian distribution function for a few representative choices of the comoving scale. Each panel shows results for counts in spherical cells with comoving radii 0.02, 0.04, 0.08, and 0.16 times the box size. For each cell size, the thin curves show the distribution of counts averaged over 30^3 cells. The two panels show results at two different expansion factors a , where $a = 1$ initially. The variance in the cell counts decreases with cell size: for the curves shown, the associated variance is 0.62, 0.11, 0.016 and 0.002 in the panel on the left, and it is 10.9, 2.1, 0.4 and 0.07 in the panel on the right.

Comparison with the linear barrier model is a little tricky. In principle, the model requires that the free parameter $\bar{\xi}_m$ of the Inverse Gaussian distribution (equation 40) should scale as $\bar{\xi}_m \propto 1/V$. In fact, although $\bar{\xi}_m$ in the simulations is $\propto 1/V$ initially, it scales differently at later times (e.g. Hamilton et al. 1991; Jain, Mo & White 1995). On large scales it is $\propto 1/V$, even at late times, but on smaller scales it is less steep. At least some of this difference between the model prediction and the simulation results is a consequence of the model assumption that haloes collapse to zero volume. This assumption means that, on scales smaller than that of a typical halo in the simulations, the model will certainly be in error. We will therefore proceed as follows. Recall that $\bar{\xi}_m$ determines the shape of the Inverse Gaussian distribution. We will assume that, on any scale V , we can treat $\bar{\xi}_m$ as a free parameter that is fixed by relating it to the value of the variance of particle counts in cells of size V measured in the simulations. This assumption allows us to test if the functional form of the Inverse Gaussian distribution provides a good description of the simulations, even if the detailed scale dependence of the model is not right.

The thick curves in Fig. 4 show Inverse Gaussian distributions that have the same variance as the distributions measured in the

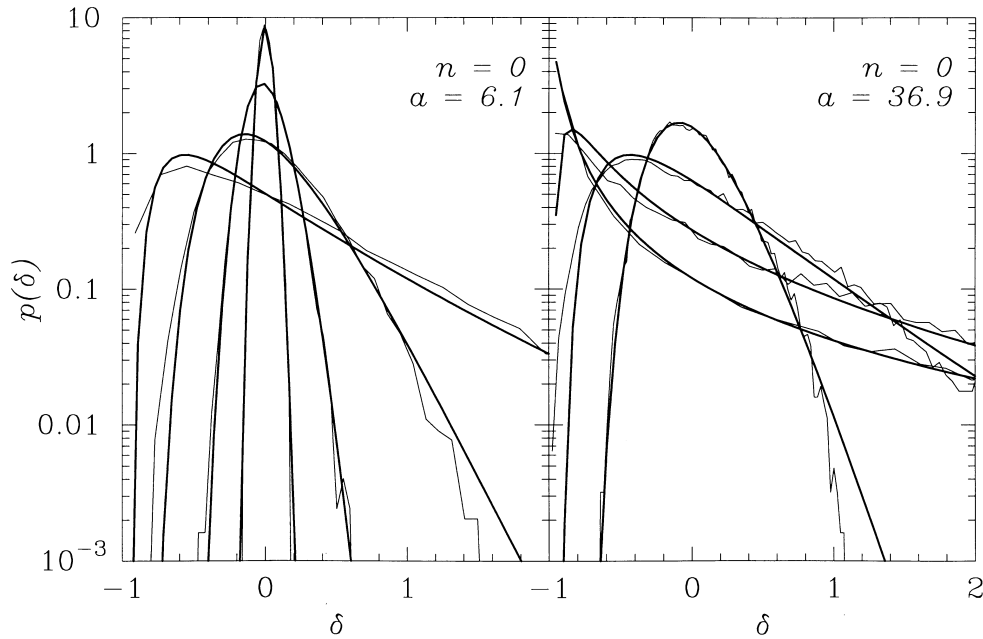


Figure 4. The Eulerian distribution function for a range of comoving scales, shown at two different output times, labelled by the expansion factor a (initially $a = 1$). Thin curves show the distribution measured in simulations of clustering from white-noise Gaussian initial conditions. Thick curves show Inverse Gaussian distributions that have the same variance as the thin curves. Larger cells have narrower distribution functions.

simulations (thin curves). When this is done, the Inverse Gaussian (equation 40) describes the simulation results reasonably well, even on small scales, at all times. In fact, the Inverse Gaussian fits $p(\delta)$ at least as well as the Press–Schechter mass function (equation 32) fits the distribution of cluster masses (see, e.g., Lacey & Cole 1994). The evolution of the variance in the simulations is reasonably well understood (Hamilton et al. 1991; Nityananda & Padmanabhan 1994; Jain et al. 1995; Padmanabhan 1996), so we could have used this to set ξ_m , rather than the simulations themselves. Fig. 4 shows that this then provides a simple way in which to extend the predictions of the linear barrier model beyond the point-cluster approximation, so that it can be applied with reasonable accuracy even on small scales.

Since the Inverse Gaussian model fits the simulation results reasonably well, the other results associated with the linear barrier model may also be of more than just academic interest. For example, in the linear barrier model, when haloes first virialize, they are uncorrelated with each other (Section 3.4). What correlations do exist arise primarily from volume exclusion effects. That is, in the initial Lagrangian space, haloes occupy a volume that is proportional to their mass. Since no other halo can occupy the region taken up by a given halo, this exclusion effect gives rise to (anti)correlations, at least on small scales. This is probably a generic consequence of the white-noise initial conditions, and is not specific to the linear barrier model.

4 DISCUSSION AND EXTENSIONS

4.1 Scaling properties of the model

The Inverse Gaussian distribution was derived here by considering the distribution of crossings of a linear barrier by Brownian motion. The relation between this barrier shape (equation 20) and that required by the spherical collapse model (equation 10) was discussed in Section 3.1.

The thick solid lines in Fig. 2 show this spherical collapse barrier (equation 10) for representative values of $V \propto R^3$. Curves for larger R , look just like those for smaller R except that are shifted to the left (since the x -axis of the plot shows the negative of the logarithm of V_0). Curves for the same comoving R but at higher redshift are simply multiplied by $(1+z)$, so the zero-crossing remains the same. Dashed curves show the corresponding quantities for the linear barrier used in Section 3. This figure shows that changing the comoving size R at fixed z is equivalent to rescaling the S_0 axis, and changing z at fixed comoving radius R is equivalent to rescaling the δ_0 axis. This provides a strong constraint on the form of the distribution of first crossings.

Namely, it implies that $f(S_0, \delta_0|R)$ should have a self-similar form, in that it should be a function of two parameters, one which is related to the scaling of the S_0 axis, and another which relates the scaling of the S_0 axis to that of the δ_0 axis. Since the first-crossing distribution is a function of only two parameters, the associated Eulerian distribution is also. It is convenient, then, to think of these parameters as being the mean and variance of the Eulerian distribution. This is an attractive feature of the model, since Colombi et al. (1997) find that, to a good approximation, the Eulerian distributions measured in N -body simulations of clustering from white-noise initial conditions are functions of the mean and the variance only.

4.2 Scale-free initial conditions

Initial Gaussian random fields with scale-free power spectra,

$P(k) \propto k^n$ with $-3 < n < 1$, are a simple generalization of white noise (for which $n = 0$). Equation (13) shows that, for these spectra,

$$S_0 \propto M_0^{-\alpha}, \quad \text{where} \quad \alpha = (n+3)/3, \quad (54)$$

which means that $\Delta = M_0/V = (S_V/S_0)^{1/\alpha}$, where $S_V \propto V^{-\alpha}$. This means that, when plotted as a function of (δ_0, S_0) , the shape of the spherical collapse barrier depends on the initial power spectrum. Although the barrier shape when $n \neq 0$ is different from that for white noise, it still has the same scaling as the white-noise barrier, since changing the Eulerian scale R is still equivalent to a simple shift of the barrier along the $\log(S_0)$ axis. So the barrier crossing and the associated Eulerian distributions will still be functions of two parameters. This is in qualitative agreement with the results of Colombi et al. (1997).

For initial conditions that are not scale-free, changing the Eulerian scale R is no longer equivalent to a simple shift of the barrier along the $\log(S_0)$ axis. Thus the barrier-crossing distribution is no longer self-similar, and the associated Eulerian distribution is no longer a function of just two parameters. Of course, two-parameter fits may remain a good approximation; at issue is the rate of change of the slope of the power spectrum over the scales at which most of the trajectories cross the barrier.

While these are encouraging features of the model, extending it to describe clustering from initial conditions that are different from white noise is not straightforward. The problem is one of ensuring correct normalization. For scale-free initial conditions, equations (54) and (16), and the requirement that the associated Eulerian distribution have unit mean (equation 4), mean that the first-crossing distributions must satisfy

$$\int_0^\infty f(S_0, \delta_0|R) dS_0 = \int_0^\infty \left(\frac{S_0}{S_V}\right)^{\frac{1}{\alpha}} f(S_0, \delta_0|R) dS_0 = 1. \quad (55)$$

The previous section showed that, for a white-noise Gaussian field, the distribution of first crossings of the linear barrier has an associated Eulerian distribution which has unit mean, as required. However, in general, not all barrier shapes are compatible with this requirement.

For example, recall that equation (11) with $\delta_{c0} = 1.5$ is a good approximation to the spherical collapse model. When $n = -1$, $\alpha = 2/3$, so the associated barrier, when written as a function of S_0 , is the same (linear) as it was in Section 3. Now, for a linear barrier, the first passage distribution is Inverse Gaussian. However, when $\alpha = 2/3$ and $f(S_0, \delta_0|R)$ is Inverse Gaussian, then the second equality of equation (55) is not satisfied. Thus it appears likely that, for arbitrary power spectra, the excursion set approach developed here will not work if at least some parametrizations of the spherical collapse barrier are used.

This means that it may be more fruitful to consider the inverse problem to that considered in this paper.

4.3 The inverse problem and the Generalized Inverse Gaussian distributions

In this paper, the barrier shape was specified, then the first-crossing distribution was obtained and, finally, the associated Eulerian distribution was derived. It may be more useful to first specify an Eulerian distribution. Then, transform it to a first-crossing distribution, from which the shape of the barrier can be inferred. This ensures that all normalization requirements have been satisfied. Once the barrier shape is known, the halo–mass and halo–halo correlations can be worked out just as they were in this paper.

Finally, this barrier shape can be compared with that required by the spherical collapse model.

In this context, it is worth mentioning that there is a class of distributions which provides convenient generalizations of the Inverse Gaussian, and may provide useful approximations to the Eulerian distributions measured in simulations of gravitational clustering from scale-free initial conditions.

The Generalized Inverse Gaussian (GIG) distribution with index λ , scale parameter η , and concentration parameter ω is

$$f_\lambda(x|\eta, \omega) dx = \frac{(x/\eta)^\lambda}{2 K_\lambda(\omega)} e^{-\frac{x}{\eta}(\frac{\omega}{x} + \frac{x}{\eta})} \frac{dx}{x}, \quad x \geq 0, \quad (56)$$

where $K_\lambda(\omega)$ is a modified Bessel function of the third kind with index λ . For a given λ , these are functions of just two parameters, η and ω , so they have the self-similar property discussed above. For these modified Bessel functions,

$$K_\lambda(\omega) = K_{-\lambda}(\omega) \quad \text{and} \quad (57)$$

$$K_{\lambda+1}(\omega) = 2(\mathcal{N}\omega) K_\lambda(\omega) + K_{\lambda-1}(\omega).$$

Therefore, when $\lambda = -(2\alpha)^{-1}$, the GIG distributions, with $x = S_0$, $\eta = S_V$ and $\omega = \delta_{c0}^2/S_V$ satisfy equation (55), so the associated Eulerian distributions are correctly normalized and have unit mean. When $n = 0$, then $\alpha = 1$, so $\lambda = -1/2$, and this distribution is the same as the Inverse Gaussian distribution considered in Section 3.

The symbols in Fig. 5 show the values of S_3 and S_4 (defined similarly to equation 42) plotted versus variance for these GIG distributions when $n = 0$ (filled circles), -1 (open circles) and -2 (stars). The curves were computed using the extended perturbation theory fitting functions of Colombi et al. (1997). The solid curves show their fits to the values of S_3 and S_4 measured in numerical simulations of clustering from the corresponding scale-free initial conditions, and dashed curves give an estimate of the allowed range of values. While the GIG values do not fit the numerical results, they do show similar trends.

The problem, then, is to determine the shape of the barrier for which the GIG distribution is the first-crossing distribution, and to then compute the associated halo distribution. The solution of this inverse problem is the subject of ongoing work, where the barriers

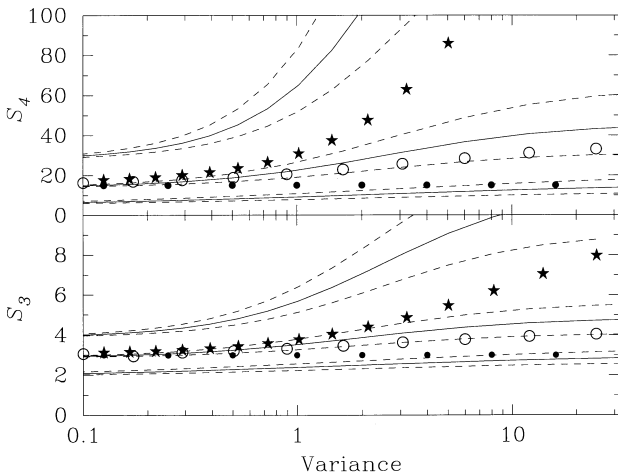


Figure 5. S_3 and S_4 versus variance for the Generalized Inverse Gaussian distributions associated with initial power spectra with slopes $n = 0$ (filled circles), -1 (open circles) and -2 (stars). The solid curves show the values measured in numerical simulations of clustering from these initial conditions, as parametrized by Colombi et al. (1997). Dashed curves show their estimates of the allowed range of values.

associated with the distributions given by the extended perturbation theory of Colombi et al. (1997) are also used as the Eulerian distributions.

5 SUMMARY

This paper develops a model that allows one to provide an approximate description of the spatial distribution of dark matter, as well as dark matter haloes, in a self-consistent way. It can also be used to estimate the evolution of the density profiles of haloes, and to quantify how matter flows in and out of Eulerian cells. The model is described in Section 2.

The model assumes that, at the epoch z , the comoving Eulerian size R of an initial Lagrangian region R_0 is related to its initial overdensity δ_0 . This assumption is motivated by the spherical collapse model. The additional assumption that the number of such regions is conserved (only their comoving size changes) allows one to compute statistics in the Eulerian space by taking appropriate averages over the relevant Lagrangian space quantities. Since the initial Lagrangian distribution can be computed (e.g. Mo & White 1996; Sheth & Lemson, in preparation), so can the Eulerian distribution. The algorithm for taking these appropriate averages is related to the solution of an excursion set, barrier-crossing problem, in which the barrier shape is given by the spherical collapse model.

A constant barrier is a special case of the barrier studied here. The first-crossing distribution associated with a constant barrier can be used to estimate the distribution of virialized halo masses (Bond et al. 1991). In the context of this paper, this special case corresponds to the limit of vanishing Eulerian cell size; the halo mass function is simply the Eulerian probability distribution function in the limit of vanishing Eulerian cell size. Thus the model here shows how the Bond et al. construction that yields the halo mass function can be extended to yield the Eulerian probability distribution function. The results of Mo & White (1996) are also easily understood within the context of this model.

In Section 3, clustering from white-noise initial conditions was considered, and the linear barrier was used to show explicitly how the model works. This was done for a number of reasons. First, the spherical collapse barrier problem must be solved numerically, whereas, for the linear barrier, most interesting quantities can be computed analytically. Secondly, within the context of this model, the linear barrier can be understood as arising from a simple variant of the spherical collapse model (Section 3.1). Finally, for this barrier shape, the associated Eulerian distribution is Inverse Gaussian (Section 3.3), and this is in good agreement with numerical simulations of clustering from white-noise initial conditions (Fig. 4).

In the white-noise, linear barrier model, correlations between haloes and mass arise from the simple fact that a cell which is known to contain a halo certainly contains that halo's mass. For the linear barrier model, the evolution of halo-halo correlations can be written analytically (Section 3.4). Correlations between haloes arise primarily from volume exclusion effects. That is, in the initial Lagrangian space, haloes occupy a volume that is proportional to their mass. Since no other halo can occupy the region taken up by a given halo, this exclusion effect gives rise to (anti)correlations, at least on small scales at early times. The effects of this volume exclusion decrease as clustering evolves. This behaviour is generic, and is not specific to the linear barrier.

Section 3.5 showed that the two-linear-barrier problem can also be solved analytically; in the model, this can be used to provide

information about the evolved density run around positions in Eulerian space. Although the necessary formulae were all derived there, we did not pursue this further.

Finally, Section 4 discussed one way in which this model could be extended to describe clustering from more general Gaussian initial conditions. The Generalized Inverse Gaussian distributions (equation 62) were introduced in this context. Strictly speaking, the model as described here is correct for $\Omega_0 = 1$ universes. It is, of course, trivial to extend it to less dense universes. Applying this model to more general initial conditions is the subject of ongoing work.

ACKNOWLEDGMENTS

I thank Houjon Mo and Simon White for providing the data from their simulations, and both of them, and Gerard Lemson, for interesting discussions.

REFERENCES

- Bernardeau F., 1994, *A&A*, 291, 697
 Bond J. R., Cole S., Efstathiou G., Kaiser N., 1991, *ApJ*, 379, 440
 Bouchet F. R., Hernquist L., 1992, *ApJ*, 400, 25
 Colombi S., Bernardeau F., Bouchet F. R., Hernquist L., 1997, *MNRAS*, 287, 241
 Cox D. R., Miller H. D., 1967, *The Theory of Stochastic Processes*. J. Wiley & Sons, New York
 Folks J. L., Chhikara R. S., 1978 *J. R. Statist. Soc. B*, 40, 263
 Fry J., 1985, *ApJ*, 289, 10
 Hamilton A. J. S., Kumar P., Lu E., Matthews A., 1991, *ApJ*, 374, L1
 Itoh M., Inagaki S., Saslaw W. C., 1993, *ApJ*, 403, 459
 Jain B., Mo H. J., White S. D. M., 1995, *MNRAS*, 276, L25
 Kao E. P. C., 1996, *An Introduction to Stochastic Processes*. Wadsworth Publishing Company, Belmont
 Lacey C., Cole S., 1993, *MNRAS*, 262, 627
 Lacey C., Cole S., 1994, *MNRAS*, 271, 676
 Mo H. J., White S. D. M., 1996, *MNRAS*, 282, 347
 Nityananda R., Padmanabhan T., 1994, *MNRAS*, 271, 976
 Padmanabhan T., 1996, in Lahav O., Terlevich E., Terlevich R., eds, *Proc. 36th Herstmonceux Conf.*, Cambridge Univ. Press, Cambridge, p. 207
 Peebles P. J. E., 1980, *The Large Scale Structure of the Universe*. Princeton Univ. Press, Princeton
 Press W., Schechter P., 1974, *ApJ*, 187, 425
 Saslaw W. C., Hamilton A. J. S., 1984, *ApJ*, 276, 13
 Schrödinger E., 1915, *Physikalische Zeitschrift*, 16, 289
 Sheth R. K., 1996a, *MNRAS*, 281, 1124
 Sheth R. K., 1996b, *MNRAS*, 281, 1277
 Sheth R. K., 1998, *MNRAS*, in press

APPENDIX A: THE FIRST PASSAGE TIME AND THE LINEAR BARRIER

This appendix presents a derivation of the first time S that a particle undergoing Brownian motion with zero drift reaches the linear barrier

$$\delta_\nu(S) = \nu - \beta S, \quad (\text{A1})$$

having started from the origin $(S, \delta) = (0, 0)$. Let $f_\nu(S)$ denote the first passage time distribution associated with this barrier. The subscript ν indicates the height of the barrier at $S = 0$.

The assumption of zero drift means that, in the absence of the absorbing barrier, the mean distance of a particle from the S axis, averaged over the ensemble of Brownian walks of the type shown in Fig. 1, is zero. To be more precise, recall that equation (27) gives the probability $p(S, \delta_0) d\delta_0$ that a trajectory has value between δ_0 and

$\delta_0 + d\delta_0$, at S . So, for those trajectories,

$$\langle \delta_0 \rangle = \int \delta_0 p(S, \delta_0) d\delta_0 = 0 \quad \text{for all } S, \quad (\text{A2})$$

and

$$\langle \delta_0^2 \rangle = \int \delta_0^2 p(S, \delta_0) d\delta_0 = S + \langle \delta_0 \rangle^2 = S \quad \text{at } S. \quad (\text{A3})$$

Since $\langle \delta_0 \rangle = 0$ for all S , these are said to be Brownian walks with zero drift.

Consider another linear barrier which is a simple shift of μ along the δ -axis of the barrier above:

$$\delta_\omega(S) = \mu + \delta_0(S) = \mu + \nu - \beta S \equiv \omega - \beta S. \quad (\text{A4})$$

Let $f_\omega(S)$ denote the first passage time distribution associated with this barrier. The subscript ω indicates the height of the barrier when $S = 0$. Then

$$f_\omega(S) dS = \int_0^S dS' f_\nu(S') f_{\omega\nu}(S|S') dS', \quad (\text{A5})$$

where $f_{\omega\nu}(S|S')$ denotes the first passage time distribution to $\delta_\omega(S)$, given that the particle started at $[S', \delta_\nu(S')]$ instead of the origin. Since the particle is undergoing Brownian motion, $f_{\omega\nu}(S|S')$ is the same as for a particle that starts at the origin, but sees a barrier

$$\delta_\mu(S) = \delta_\omega(S) - \delta_\nu(S') = \mu - \beta(S - S'). \quad (\text{A6})$$

So we can write

$$f_{\omega\nu}(S|S') = f_\mu(S - S'), \quad (\text{A7})$$

where the subscript μ indicates that the height of the barrier above the starting position at S' is μ .

This means that equation (A5) is a convolution equation:

$$f_\omega(S) = f_{\mu+\nu}(S) = \int_0^S f_\nu(S') f_\mu(S - S') dS'. \quad (\text{A8})$$

When $\beta = 0$, then the barrier is constant, and the first passage distribution is known to be

$$f_\nu(S) dS = \left(\frac{\nu^2}{2\pi S} \right)^{1/2} e^{-\nu^2/2S} \frac{dS}{S}. \quad (\text{A9})$$

It is straightforward to verify that this expression satisfies the convolution equation above. Therefore the solution to the convolution equation when $\beta \neq 0$ must be

$$f_\nu(S) dS = \left(\frac{\nu^2}{2\pi S} \right)^{1/2} e^{-(\nu-\beta S)^2/2S} \frac{dS}{S}. \quad (\text{A10})$$

A more formal derivation can be found in e. g., Schrödinger (1915) or Cox & Miller (1967). The following derivation follows that in Kao (1996) closely.

First, multiply both sides of equation (A5) by $\exp(-tS)$, and integrate over all S . This gives the Laplace transform $\mathcal{L}(\omega, t)$ of $f_\omega(S)$. Equation (A5) implies that

$$\begin{aligned} \mathcal{L}(\omega, t) &= \int_0^\infty dS e^{-tS} \int_0^S dS' f_\nu(S') f_{\omega\nu}(S|S') \\ &= \int_0^\infty dS' f_\nu(S') \int_{S'}^\infty dS f_\mu(S - S') e^{-tS} \\ &= \int_0^\infty dS' f_\nu(S') e^{-tS'} \int_0^\infty dS'' f_\mu(S'') e^{-tS''} \\ &= \mathcal{L}(\nu, t) \mathcal{L}(\mu, t), \end{aligned} \quad (\text{A11})$$

which is the same as

$$\mathcal{L}(\nu + \mu, t) = \mathcal{L}(\nu, t) \mathcal{L}(\mu, t). \quad (\text{A12})$$

This is a functional equation with solution $\mathcal{L}(\nu) = e^{-C\nu}$, where $C > 0$ is some constant, and we have not bothered to write the dummy variable t . The problem, then, is to find C .

To do so, notice that the crossing of a barrier which decreases as S increases, by Brownian walks with zero drift, is equivalent to the crossing of a constant barrier by trajectories that, in the mean, drift upwards as S increases, provided that the drift is chosen correctly. This correct choice of drift corresponds to choosing

$$\langle \delta_0 \rangle \equiv \beta S \quad \text{at } S. \quad (\text{A13})$$

Of course, the variance remains the same, so that

$$\langle \delta_0^2 \rangle = S + \langle \delta_0 \rangle^2 = S + \beta^2 S^2 \quad \text{at } S. \quad (\text{A14})$$

So the problem of the crossing of the linear barrier $\delta_\nu(S) = \nu - \beta S$ by walks with zero drift is transformed to the problem of the crossing of a constant barrier of height ν by walks with upward drift β . In particular, the relation (A12) remains the same.

So, to find C , assume that the probability of first crossing the barrier ν in the first small increment s along the S axis is negligible. Suppose that at $S = s$, the random trajectory has value $\delta_0 < \nu$. Then

$$\begin{aligned} f_\nu(S) &= \int f_\nu(S|\delta_0, s) p(s, \delta_0) d\delta_0 \\ &= \int_{f_{\nu-\delta_0}} (S-s) p(s, \delta_0) d\delta_0, \end{aligned} \quad (\text{A15})$$

so that

$$\begin{aligned} \mathcal{L}(\nu, t) &= \int_0^\infty dS e^{-tS} \int f_{\nu-\delta_0}(S-s) p(s, \delta_0) d\delta_0 \\ &= \int d\delta_0 p(s, \delta_0) \int_s^\infty dS f_{\nu-\delta_0}(S-s) e^{-tS} \\ &= e^{-ts} \int d\delta_0 p(s, \delta_0) \mathcal{L}(\nu - \delta_0, t). \end{aligned} \quad (\text{A16})$$

In what follows, we will sometimes omit the dummy variable t : $\mathcal{L}(\nu) \equiv \mathcal{L}(\nu, t)$. As s and δ_0 are small,

$$\mathcal{L}(\nu - \delta_0) \approx \mathcal{L}(\nu) - \delta_0 \mathcal{L}'(\nu) + \frac{\delta_0^2}{2} \mathcal{L}''(\nu), \quad (\text{A17})$$

and

$$e^{-ts} \approx 1 - ts. \quad (\text{A18})$$

These expressions imply that

$$\begin{aligned} \mathcal{L}(\nu) &\approx (1 - ts) \left[\mathcal{L}(\nu) - \langle \delta_0 \rangle \mathcal{L}'(\nu) + \frac{\langle \delta_0^2 \rangle}{2} \mathcal{L}''(\nu) \right] \\ &= (1 - ts) \left[\mathcal{L}(\nu) - \beta s \mathcal{L}'(\nu) + \frac{s + (\beta s)^2}{2} \mathcal{L}''(\nu) \right] \\ &\approx \mathcal{L}(\nu) - ts \mathcal{L}(\nu) - \beta s \mathcal{L}'(\nu) + \frac{s}{2} \mathcal{L}''(\nu), \end{aligned} \quad (\text{A19})$$

The second line follows from (A13) and (A14), and the third is correct to lowest order in s . Dividing by s , and taking the limit $s \rightarrow 0$, reduces this to

$$t \mathcal{L}(\nu) = -\beta \mathcal{L}'(\nu) + \frac{1}{2} \mathcal{L}''(\nu). \quad (\text{A20})$$

However,

$$\mathcal{L}(\nu) = e^{-C\nu}, \quad \text{so } \mathcal{L}'(\nu) = -C e^{-C\nu}, \quad \text{and } \mathcal{L}''(\nu) = C^2 e^{-C\nu}.$$

These expressions in (A20) imply that

$$C^2 + 2\beta C - 2t = 0, \quad (\text{A21})$$

so that, if $C > 0$, then

$$C = -\beta + \sqrt{\beta^2 + 2t}, \quad (\text{A22})$$

since β and t are both positive. Thus

$$\mathcal{L}(\nu, t) = e^{\nu\beta - \nu\sqrt{\beta^2 + 2t}}. \quad (\text{A23})$$

Inverting this Laplace transform gives the Inverse Gaussian distribution.

This problem can also be formulated in the context of the diffusion equation. In the notation of Lacey & Cole (1993), the associated diffusion equation is

$$\frac{\partial Q}{\partial S} = -\beta \frac{\partial Q}{\partial \delta} + \frac{1}{2} \frac{\partial^2 Q}{\partial \delta^2}, \quad (\text{A24})$$

where β is the drift term, and $Q(S, \delta, \nu)$ represents the solution to this equation in the presence of an absorbing boundary at $\delta = \nu$. Bond et al. (1991) and Lacey & Cole (1993) considered the case $\beta = 0$.

This paper has been typeset from a $\text{T}_\text{E}\text{X}/\text{L}^\text{A}\text{T}_\text{E}\text{X}$ file prepared by the author.